Reactivating aversive memories in humans: An EEG and Microstates study of post-retrieval processes

Luciano Cavallino[1], Luz Bavassi[1], Maria Eugenia Pedreira[1#]

[1°] Laboratorio de Neurociencias de la memoria, Instituto de Fisiología, Biología Molecular y Neurociencias (IFIBYNE), CONICET, Facultad de Ciencias Exactas y Naturales, Universidad de Buenos Aires, Buenos Aires, Argentina.

[#] Corresponding author
Maria Eugenia Pedreira, Ph.D. Laboratorio de Neurociencias de la memoria, Instituto de Fisiología, Biología Molecular y Neurociencias (IFIBYNE, CONICET), Facultad de Ciencias Exactas y Naturales, Universidad de Buenos Aires. Av. Costanera Rafael Obligado, Ciudad Universitaria, Ciudad Autónoma de Buenos Aires, (C1428EGA), Buenos Aires, Argentina. E-mail: mariaepedreira@gmail.com

Abstract

Although fear conditioning is one of the most widely used models to study anxiety in humans, much remains to be explored regarding its underlying neural correlates. It is known that the retrieval of consolidated memories can trigger modifications—weakening, strengthening, or updating of the original memory—depending on the cues presented during the reminder.

In this study, we employed a three-day threat-conditioning protocol in which an angry face (conditioned stimulus, CS+) was paired with an aversive sound (unconditioned stimulus, US). Our main objective was to identify neural markers of post-retrieval processes triggered by the presentation of the CS+ alone, 24 hours after acquisition. Additionally, we aimed to assess cognitive biases by examining how the perception of the conditioned stimulus changes following conditioning.

To this end, we recorded resting-state electroencephalographic (EEG) activity using a 30-channel system at a 256 Hz sampling rate. We analyzed four minutes of resting-state EEG following the presentation of the reminder cue, focusing on memory-related patterns in the frequency domain and microstate dynamics. We compared neural activity after the reminder presentation between two groups: a Reactivation group previously exposed to threat conditioning on the first day and a Control group with no prior conditioning.

Our results confirmed successful conditioning (CS+–US association) and memory retention 48 hours later, as evidenced by higher skin conductance responses and greater US expectancy to the CS+. Moreover, participants rated the CS+ face as more aversive than the CS− face 48 hours after conditioning, compared to their pre-conditioning ratings. Relative to the Control group, the Reactivation group showed decreased beta-band activity (25–30 Hz) in central regions during the 90 seconds following the reminder, which may reflect enhanced post-reactivation processing of the memory, in contrast to participants who saw the face for the first time. Previous research has highlighted the role of reduced beta amplitude in the encoding and retrieval of another type of memory: episodic memory. Furthermore, when analyzing EEG microstates (short-lived, quasi-stable topographies of brain activity that reoccur over time), we found lower global field power for microstates C, A, E, and B in the Reactivation group compared with the Control group.

Our findings provide initial evidence for neural correlates associated with post-retrieval processes, including decreased beta activity and microstate-level differences related to the post-retrieval processing of an implicit memory.

Introduction

Understanding environmental threats serves as a critical survival mechanism, allowing organisms to associate previously neutral stimuli with aversive events. This leads to the formation of implicit memories that initiate defensive behaviors, thereby helping to prevent direct harm and enhancing survival rates (Fanselow, 2018). However, when an organism fails to suppress threat responses in safe environments, these survival behaviors can become maladaptive, resulting in dysfunctional reactions. Many researchers propose that these mechanisms may contribute to anxiety disorders (Grupe & Nitschke, 2013). In this context, threat-conditioning paradigms offer a powerful experimental approach for investigating the neurobiological foundations of anxiety disorders. Foundational studies in animal models have identified the amygdala as a central hub for the associative learning of neutral cues and aversive outcomes (LeDoux, 2000; Davis, 1992; Rogan et al., 1997; Fanselow & Poulos, 2005). In humans, threat conditioning demonstrates that skin conductance responses are indicative of autonomic nervous system activity (Sjouwerman & Lonsdorf, 2018), acting as a reliable marker for the implicit expression of threat memories, even in the absence of conscious awareness of the underlying contingencies (Öhman & Mineka, 2001; Phelps & LeDoux, 2005; Raio et al., 2012). Clinical studies further illustrate that altered threat conditioning and extinction processes are characteristic of anxiety disorders, thus linking fundamental mechanisms of associative learning to psychopathology (Grillon, 2002; Lissek et al., 2005; Milad & Quirk, 2012). Collectively, this body of research has established threat conditioning as a cross-species model that connects conserved neural and physiological processes with maladaptive fear and anxiety.

The resurgence of experiments suggesting that specific cues can trigger the reactivation of memories has called into question the longstanding assumption that consolidated memories are permanently resistant to modification (Nader et al., 2000; Alberini, 2005). This has led to the development of the reconsolidation framework, which posits that the presentation of a reminder triggers reactivation and acts as a mechanism facilitating memory malleability. A closer examination of these protocols reveals that the effectiveness of these reminders relies on the presentation of partial information from the original task. In general, incomplete reminders are characterized by the omission of the expected outcome. However, a deeper analysis of the reminder structures indicates that their effectiveness relies on providing cues that contain critical information, thereby prompting attempts at retrieval (Forcato, 2009; Fernandez, 2016). In the context of TC paradigms, which are more common for both animals and humans, the reminders typically involve the omission of the unconditioned stimulus (US) (Nader et al., 2000; Kindt et al., 2009).

Anxiety disorders involve physiological, emotional, and cognitive alterations. However, experimental paradigms typically focus on associative responses

assessed through autonomic indices (e.g., heart rate variability, skin conductance) and declarative measures (e.g., contingency awareness). This emphasis neglects key components of threat processing, such as cognitive bias, defined as systematic deviations from rational judgment (Tversky & Kahneman, 1974; Leung et al., 2022). To bridge this gap, we developed a protocol that integrates physiological and declarative measures with tasks revealing cognitive bias, providing a novel tool to investigate cognitive disturbances associated with anxiety disorders (Fernandez et al., 2018). More recently, we demonstrated that the presentation of a prediction error reminder (CS+ without US) 24 hours after conditioning led to the labilization of the previously formed memory in a threat conditioning paradigm (Picco et al., 2022). This conclusion was based on findings that performing a highly demanding task immediately after memory reactivation eliminated the increased SCR to the CS+ during testing and abolished the cognitive bias effect. These results support the idea that the demanding task weakened the memory trace, but only when the memory had first been reactivated and rendered labile by the reminder.

Given that memory processes rely on neural communication and plasticity across a broad range of timescales, it has been proposed that oscillatory brain activity, ranging from milliseconds to seconds, carries information about higher-order cognitive processes, both in terms of amplitude dynamics and phase coherence (Lakatos et al., 2005). For example, it has been demonstrated that decreases in amplitude within the 8–40 Hz frequency range play an active role in the formation and retrieval of long-term episodic memories (Hanslmayr et al., 2012). Furthermore, in recent years, the use of microstate analysis has significantly increased in the search for neural markers associated with various mental processes (Tarailis et al., 2024). Microstates are short-lived, quasi-stable topographies of brain activity (lasting approximately 80–120 ms) that reoccur over time (Lehmann et al., 1987; Koenig et al., 2002). They have been proposed as fundamental building blocks of information processing in the brain (Lehmann, 1990; Koenig et al., 2002). Four canonical microstates were defined according to their topography as Microstate A, B, C, and D (Koenig et al., 2002). These same microstates have been consistently identified in a wide range of studies involving different cognitive processes (Tarailis et al., 2024), and were also found in the present study.

Building on this foundation, the present study aimed to identify neural markers associated with the post-reactivation phase of threat-conditioned memories. Employing a three-day threat-conditioning protocol alongside EEG recordings taken during resting states before and after the reminder presentation, we investigated both oscillatory dynamics and microstate organization to capture the rapid neural processes associated with memory reactivation.
Our results demonstrated successful threat conditioning in this paradigm, as evidenced by declarative memory responses, implicit physiological responses, and cognitive biases. Furthermore, we observed differences in brain activity during the eye-close resting state depending on whether participants had previously undergone

conditioning (Reminder reactivated a previously formed memory), or whether the stimulus was novel and thus no memory was available for reactivation. Specifically, we found a lower beta-band activity (25–30 Hz) in the reactivation group compared to the control group, highlighting the relevance of oscillatory activity in this frequency range for post-reactivation processes of threat-conditioned memories. Additionally, our findings suggest a potential key role for microstates C, A, and E in the neural dynamics underlying these processes. This integrative approach provides new insights into the mechanisms through which reactivated threat memories are stabilized or modified, offering a framework for a deeper understanding of the neural basis of memory reactivation in relation to memory updating. This preliminary evidence suggests that adaptive updating mechanisms may offer new pathways to comprehend why, under certain circumstances, they fail to promote flexible regulation of aversive memories.

Material and methods

Before the experiment, all participants provided written informed consent, approved by the Ethics Committee of the Review Board of the Sociedad Argentina de Investigación Clínica (SAIC, Protocol #02/16), following the Declaration of Helsinki. A total of 52 participants between 18 and 35 years old were included (23 males and 29 females, mean age = 22.92 ± 0.54 years). Three other subjects were excluded from the analysis due to technical problems with the EEG recordings. Participants were randomly assigned to one of two groups, each comprising 26 individuals: Control group (15 females and 11 males, 23.03 ± 0.84 years) and Reactivation group (14 females and 12 males, 22.08 ± 0.70 years).

Subjective Assessment

The State-Trait Anxiety Inventory (STAI-S and STAI-T) (Spielberger, 1970) and the Beck Anxiety Inventory (BAI) (Beck et al., 1990) questionnaires were administered to assess participants' anxiety and depressive levels, as these may affect fear conditioning, particularly threat conditioning (Boddez et al., 2012; Browning et al., 2015). Participants scoring above STAI > 45 or BAI > 30 were excluded; however, no participants were excluded based on these criteria.

Experimental protocol

Reactivation Group

Participants assigned to the reactivation group completed a three-day consecutive experiment. On Day 1, they performed Stimuli Representation 1 followed by the threat conditioning. Twenty-four hours later (Day 2), a 4-minute resting-state EEG was recorded prior to stimulus presentation (Rest 1). After the incomplete reminder was presented (CS+ without the tone), a second resting-state EEG was recorded (Rest 2). On Day 3, memory evaluation (Test) was performed followed by Stimuli

Representation 2 (Figure 1). Finally, a Valuation task (probability and cost) was completed.

Control Group

Participants in the control group only completed the Day 2 task: a 4-minute resting-state EEG was recorded before stimulus presentation (Rest 1). After the incomplete reminder was presented, a second resting-state EEG was recorded (Rest 2) (Figure 1).

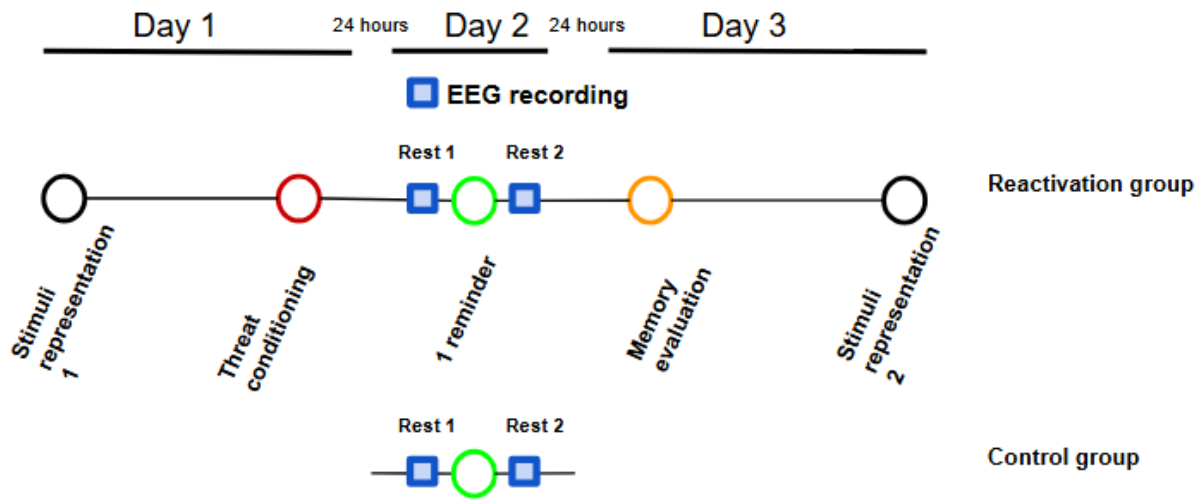

Figure 1. Schematic depiction of the experimental design illustrating group specifications across the three experimental sessions. Chronological outline of the experimental schedule for the two groups: Reactivation Group: performed the tasks across all three days, with a reminder of the CS previously paired with the US presented on the second day. Control Group: performed only the second-day task, observing the same reminder, but for them it was the first time encountering it

Cognitive Bias

Stimuli Representation: Participants rated the aversiveness of 12 different male faces (seven angry and five neutral) on a 0–8 scale. Pictures were presented randomly and centrally on a black screen (each measuring 9.5 cm × 7 cm) until a response was given on the keyboard. Stimuli Representation 1 was performed before conditioning on Day 1, and Stimuli Representation 2 was performed after conditioning on Day 3.

Valuation (Probability and Cost): The angry faces used as CS+ and CS– in threat conditioning were presented similarly to Stimuli Representation, but each was associated with a hypothetical scenario. For each stimulus, 24 positive and 24 negative scenarios were presented. Participants first rated the probability that the face was associated with the scenario (0–8 scale), then rated the aversiveness or desirability of the scenario (0–8 scale). An example of hypothetical situations and pictures is provided in Supplementary Material 1.

Threat Conditioning

Following a paradigm similar to Picco et al., 2022, two aversive (CS+ and CS–) and one neutral (CSn) male faces were presented centrally on a black screen (each slide measuring 9.5 cm × 7 cm) as conditioned stimuli. CS+ and CS– pictures were counterbalanced across participants. The unconditioned stimulus (US) was a 1.5-second auditory tone delivered through stereo headphones, generated by a TG/WN Tone-Noise Generator (Psychlab) and digitally controlled to maintain a mean intensity of 98 dB ± 2 dB. For each participant, US intensity was individually set to evoke an unpleasant but not painful sensation.

Acquisition phase: On Day 1, each face was presented 8 times in different order (see Supplementary Material 2). Each trial consisted of a 6-second face presentation followed by a black screen inter-trial interval of 8–12 seconds randomly assigned. The CS+ was paired with the US (tone) on 75% of presentations, overlapping the last 1.5 seconds of the CS. CS– and CSn were never paired with the tone.

Reactivation phase: On Day 2, the CS+ face (previously paired with the tone) was presented as before, but at the time the tone would have occurred, a screen indicating the end of the experiment was shown and no tone was delivered.

Memory evaluation (Test): On Day 3, one trial of each face (CS+, CS–, CSn) was presented as in the acquisition phase, but without the tone.

During acquisition and memory evaluation, US expectancy and Skin Conductance Response (SCR) were measured as described below. All faces used in this experiment were taken from the Karolinska Directed Emotional Faces database.

Measurements

US Expectancy:

Participants responded “YES” or “NO” using a two-button keyboard, indicating whether they expected the tone to follow the presented face. Responses were considered valid only if made within the first 4.5 seconds post CS presentation (time interval preceding the US presentation).

Implicit Response:

Sympathetic arousal was assessed via the rapid phasic components of electrodermal activity, specifically Skin Conductance Response (SCR), which reflects the emotional and cognitive states triggered by the CS (Braithwaite et al., 2013). The literature suggests that the effects of a stimulus on SCR are typically observed between 1 and 4 seconds post-stimulus (Braithwaite et al., 2013; Sjouwerman & Lonsdorf, 2019). This involuntary physiological response reflects the level of

excitability induced by different stimuli. When a stimulus (CS+) is paired with an aversive stimulus (US), the presentation of the CS+ generates an anticipation of the upcoming US, which increases arousal and may lead to an enhanced SCR. This effect has been previously observed in threat-conditioning studies (Boucsein et al., 2012, Fernandez et al., 2018, Picco et al., 2022). SCR was recorded using a Psychlab Precision Contact Instruments device with a 50 Hz sine excitation voltage (±0.5 V). Two Ag/AgCl electrodes (20 mm × 16 mm) were placed on the intermediate phalanges of the index and middle fingers of the non-dominant hand. The baseline was defined as the mean conductance during the first 0.5 seconds after CS onset. SCR was calculated as the difference between this baseline and the mean conductance between 0.5 and 4.5 seconds post-CS. A five-point moving average filter was applied to smooth the raw SCR signal. Each participant thus had one SCR value per trial (27 total: Acquisition : 8 CS+, 8 CS–, 8 CSn; Test –:1 CS+, 1 CS–, 1 CSn). SCR values were standardized into z-scores by subtracting the participant's mean and dividing by the standard deviation.

EEG preprocessing

Four minute eyes-closed resting-state EEG was recorded for each participant before (Rest 1) and after (Rest 2) stimulus presentation. Given that the most robust results were observed during the last 90 seconds of Rest 1 and the first 90 seconds of Rest 2, this time interval was used for subsequent analyses. EEG was recorded using an Akonic Bio-PC 30 cap-mounted tin electrode system (10/20 international system, Electro-Cap International Inc.), referenced to the average of the two mastoids, sampled at 256 Hz. Data were bandpass filtered between 1 and 35 Hz (8th order Butterworth filter) and re-referenced to the average of all channels. Ocular artifacts were removed using independent component analysis (ICA), and erratic or deviating channels were visually inspected and interpolated as necessary. Data were discarded if more than three channels required interpolation. Time-frequency decomposition was performed using 7-cycle Morlet wavelets between 3 and 30 Hz. For each participant, Rest 2 data were baseline-corrected by division with the time-averaged Rest 1 data.

Microstate Analysis

Microstate analysis was performed using the Microstate EEGLAB toolbox (Poulsen et al., 2018). After preprocessing (filtering, ICA, interpolation), Rest 1 and Rest 2 data from both groups were combined to generate microstate prototypes.
The Global Field Power (GFP) was computed at each time point as the standard deviation of the potentials across electrodes, providing a reference-free measure of the overall strength of the electric field at the scalp. Specifically, GFP was calculated as shown in equation 1:

$$\mathrm{GFP}(t) = \sqrt{\frac{1}{N-1}\sum_{i=1}^{N}(V_i(t) - \bar{V}(t))^2}$$

Equation 1: N: total number of electrodes (channels); V_i (t): voltage recorded at electrode i at time point t; and the average voltage across all electrodes at time point t.

Global Field Power (GFP) was calculated across all channels and frequencies between 3 and 30 Hz. Peaks of local GFP maxima (1000 peaks per participant, minimum 10 ms apart; peaks exceeding 1 standard deviation of GFP values were excluded) were used for clustering. A modified K-means algorithm with 50 random initializations optimized cluster number by minimizing cross-validation criteria (Equation 2, Poulsen et al., 2018). Microstates were ordered by decreasing GEV (Equation 3, Poulsen et al., 2018) and labeled according to canonical microstates (Koening et al., 2002): Microstate C (symmetric anterior-posterior configuration, GEV = 0.26), Microstate A (right frontal-left posterior, GEV = 0.15), Microstate E (posterior-central peak, GEV = 0.14), and Microstate B (left frontal-right posterior, GEV = 0.10) The optimal number of clusters was 4 (CV = 26.4, GEV = 0.64) (Figure 2).

$$\mathrm{CV} = \hat{\sigma}^2 \cdot \left(\frac{C-1}{C-K-1}\right)^2$$

Equation 2. C: Number of EEG channels; K: number of microstates clusters; $\hat{\sigma}^2$ an estimator of the variance of the residual noise.

$$\mathrm{GEV}_n = \frac{(\mathrm{Corr}(\mathbf{x}_n, \mathbf{a}_{l_n}) \cdot \mathrm{GFP}_n)^2}{\sum_{n'}^{N} \mathrm{GFP}_{n'}^2}$$

Equation 3. Correlation between EEG sample (x) and its assigned prototype (a). GFP was calculated as in Equation 1.

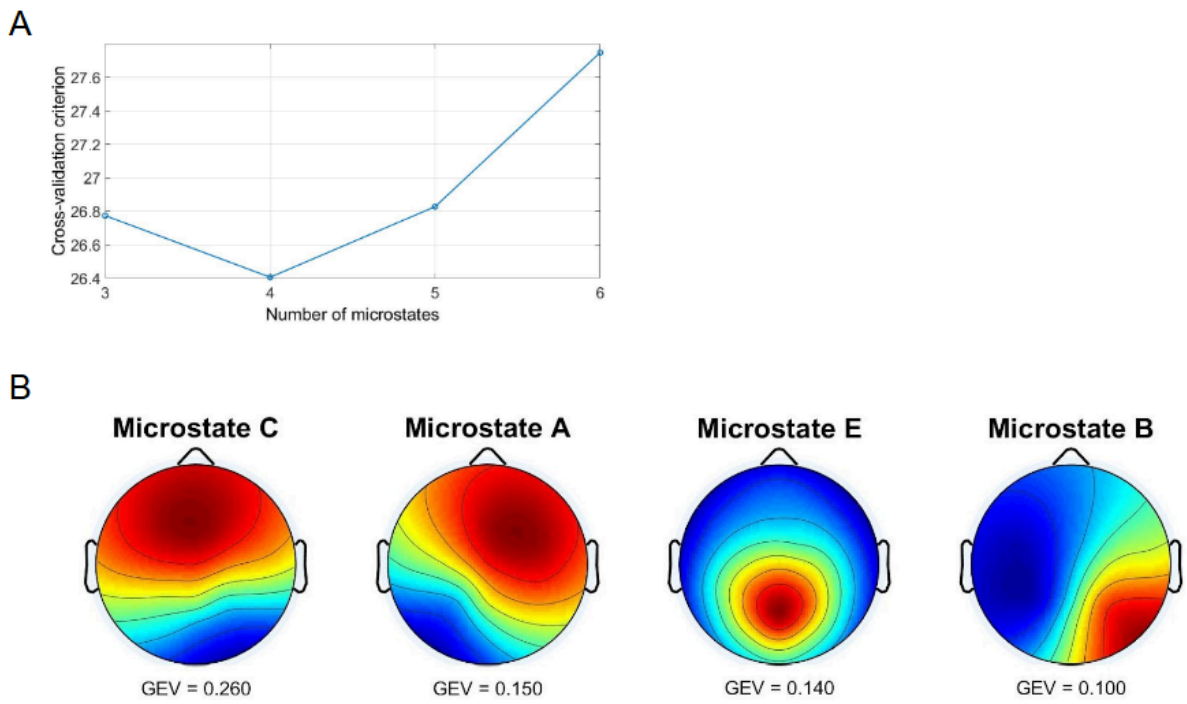

Figure 2. A) The CV was calculated for 3, 4, 5, and 6 microstates, yielding an optimal number of 4 microstates that minimized the CV. These are presented in B) Microstate prototypes ordered in decreasing GEV. They were labeled as C, A, E and B according to Tarailis et al. (2020).

Statistical Analysis

US Expectancy:

Because including participant as a random effect did not improve model fit, a generalized logistic regression model was used without random effects. Due to quasi-complete or complete separation in some conditions (all participants responding “yes” or “no”), odds ratios of responding “YES” were estimated using Firth’s penalized likelihood method (logistf package in R), which provides bias-reduced estimates and valid inference when standard logistic regression fails. Results are presented as odds ratios (OR), comparing the probability of responding "yes" for each stimulus against the probability of responding "yes" to the CS+. OR values greater than 1 indicate that the likelihood of a "yes" response to the compared stimulus is higher than to the CS+, whereas OR values less than 1 indicate a lower likelihood compared to the CS+.

Implicit Response:

To analyze the effect of stimulus type (CS+, CS–, CSn) on z-scored SCR for each trial, a repeated-measures ANOVA was conducted using R’s base aov function. The error structure accounted for the within-subject design (Error(Participant/stimulus)). Post hoc pairwise comparisons were performed using estimated marginal means (EMMs) with the emmeans package. Model assumptions were checked: residual

normality (Shapiro-Wilk test and Q-Q plots), sphericity (Mauchly's test via afex's aov_ez function), and homogeneity of variances (Levene's test from car package). Outliers were removed prior to analysis. All assumptions were met (see Supplementary Table 1).

Cognitive Bias:

Ordinal responses (Aversiveness scores) were analyzed using cumulative link mixed models (CLMM) via the ordinal package. Fixed effects included Time (Stimuli Representation 1 vs 2), Stimulus (CSs), and their interaction; participant was included as a random intercept. Estimated marginal means for interactions were computed with emmeans, and pairwise comparisons used Tukey's correction. Assumptions were tested: multicollinearity was assessed via Variance Inflation Factors (VIF < 5 acceptable), and the proportional odds assumption was tested using the nominal_test() function on a model without random effects. (see Supplementary table 2).

EEG Time-Frequency Analysis:

Time-frequency data were compared between Rest 1 and Rest 2 within groups using non-parametric cluster-based permutation tests (FieldTrip toolbox; Oostenveld et al., 2011). Monte Carlo methods with 1000 randomizations controlled for multiple comparisons by clustering electrodes with consistent differences. Two-sided dependent samples t-tests compared Rest 1 vs Rest 2 (cluster alpha = 0.05, minimum two neighboring channels per cluster, significance $p < 0.05$). Data were averaged over time.
Between-group comparisons (Reactivation vs Control, Rest 2 normalized by Rest 1 baseline) were performed using independent t-tests.
Both analyses were conducted on the last 90 seconds of Rest 1 and the first 90 seconds of Rest 2.

Microstate Analysis:

After deriving microstate prototypes, statistics were calculated per participant including Global Explained Variance (GEV), Global Field Power (GFP), duration, coverage, and occurrence. After removing outliers, these variables were analyzed per microstate using linear mixed-effects models with Rest (1 vs 2), Group (Control vs Reactivation), and their interaction as fixed effects, and participant as a random effect. Significant interactions were followed up with post hoc tests using EMMs. Model assumptions (normality and homoscedasticity) were checked via residual diagnostics (Q–Q plots, residuals vs fitted plots). No major deviations were found. Within the Reactivation group, participants were classified into two subgroups using k-means clustering (k = 2) based on standardized differences in evaluative scores and skin conductance responses (CS+ minus CS−) during testing, with the aim of comparing microstate measures between subgroups differing in their behavioral responses.

Results

US expectancy:

The proportion of "yes" responses (indicating that the US was expected following the CS) was significantly higher for CS+ compared to CS− and CSn starting from Trial 2 of the acquisition phase, and this difference persisted throughout the acquisition and into the test phase.

During Trial 1, no significant difference was found in the proportion of "yes" responses to CS+ (46%) versus CS− (30%) (Odds Ratio (OR) = 0.53, 95% CI [0.17, 1.60], $p = 0.26$). However, a higher proportion of "yes" responses was observed for CS+ compared to CSn (0%) (OR = 0.028, 95% CI [0.0002, 0.25], $p < 0.001$).

By the end of the acquisition phase, in Trial 8, a marked difference emerged, with 100% of participants responding "yes" to CS+ compared to 0% for both CS− and CSn (OR = 0.00035, 95% CI [0.0000011, 0.0073], $p < 0.001$).

A similar pattern was observed during the memory retention test phase: the proportion of "yes" responses to CS+ was 92%, compared to 7% for CS− (OR = 0.0065, 95% CI [0.0005, 0.041], $p < 0.001$) and 4% for CSn (OR = 0.0038, 95% CI [0.0002, 0.028], $p < 0.001$) (Figure 3a).

Implicit response:

A successfully threat conditioning was observed, as evidenced by a greater skin conductance response (SCR) to the CS+ during the late phases of acquisition and the memory retention test, a difference that was not present during the early phases of acquisition (Figure 3b)

To evaluate the implicit response during threat conditioning acquisition, we compared SCR (Z-score) between stimuli (CS+, CS–, and CSn) during the early phase of acquisition (Trials 1 and 2) and the late phase (Trials 7 and 8). We found that during the early phase, there were no significant differences between stimuli. However, by the end of acquisition, SCR was significantly higher for CS+ compared to CS– and CSn, highlighting the effect of conditioning on sympathetic arousal.
Early phase (Trial 1 and 2): The main effect of stimulus was not significant, $F(2, 40) = 0.62$, $p = 0.542$. Figure 3 c
Late phase (Trial 7 and 8). A significant effect of stimulus was found, $F(2, 46) = 5.66$, $p = 0.0063$. Post hoc pairwise comparisons (adjusted for multiple testing): The estimated mean difference between CS1 and CS2 was 0.39 (SE = 0.13), $t(46) = 2.96$, $p = 0.013$; between CS1 and CS3 it was 0.38 (SE = 0.13), $t(46) = 2.86$, $p = 0.016$; and between CS2 and CS3 it was -0.01 (SE = 0.13), $t(46) = -0.09$, $p = 0.995$. Figure 3 d

To evaluate implicit memory retention, we compared SCR (Z-score) between stimuli (CS+, CS–, and CSn) during the day 3 (Test). We found a successfully memory retention, evidenced for the higher SCR (Z-score) of the CS+ compared with the CS- and CSn. A significant effect of stimulus was found $F(2, 46) = 4.38$, $p = 0.018$. Post hoc pairwise comparisons (adjusted for multiple testing): The estimated mean difference between CS1 and CS2 was 0.53 (SE = 0.21), $t(46) = 2.53$, $p = 0.038$; between CS1 and CS3 it was 0.54 (SE = 0.21), $t(46) = 2.59$, $p = 0.033$; and between CS2 and CS3 it was 0.01 (SE = 0.21), $t(46) = 0.052$, $p = 0.998$. Figure 3e

Cognitive bias:

In order to evaluate cognitive bias associated with threat conditioning, we compared the aversiveness score of the CS+ and CS- before and after conditioning. We found that after conditioning only the CS+ was rated as more aversive/unpleasant, meanwhile the aversive score of the CS- did not change, highlighting the effect of the association between that particular image (CS+) and the aversive tone onto the aversive perception of the face.

The interaction between Representation (1 and 2) and stimulus (CS+ and CS-) was statistically significant ($\beta = 2.41$, SE = 0.75, $z = 3.19$, $p = 0.001$), suggesting that the effect of stimulus differed by representation. Neither the main effect of Stimulus ($\beta = -0.34$, $p = 0.484$) nor Representation alone ($\beta = -0.86$, $p = 0.095$) reached statistical significance. Meanwhile no differences were found before and after conditioning for the CS- (Estimate 0.85, SE = 0.51, $z = 1.67$, n=26, $p = 0.339$) the aversiveness score was higher after conditioning for the CS+ (Estimate -1.55, SE = 0.52, $z = -2.96$, n=26, $p = 0.015$). Furthermore, the aversiveness score of the representation 2 was higher for the CS+ compared with the CS- (Estimate -2.06, SE = 0.55, $z = -3.72$, $p = 0.001$) a differences not found for the representation 1 (Estimate 0.34,SE = 0.49, $z = 0.70$, $p = 0.89$) Figure 3f.

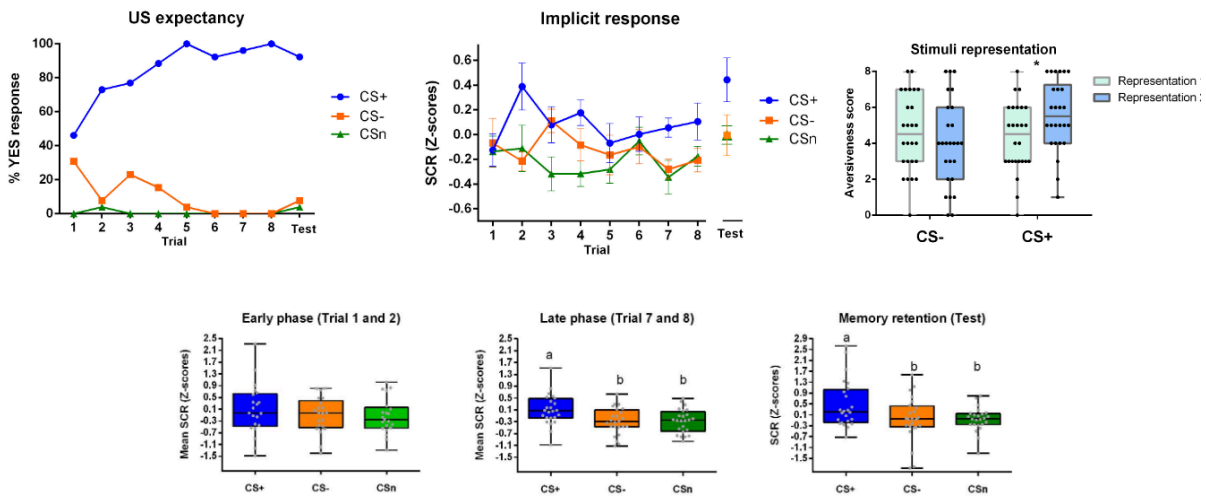

Figure 3. A) US expectancy represented as the proportion of “Yes” responses (“I will hear the tone after the CS”) for the three stimuli (CS+, CS–, CSn) across the 8 conditioning trials and the test trial,

48 h later. B) Skin Conductance Response (z-scored) for the three stimuli (CS+, CS–, CSn) across the 8 conditioning trials and the test trial, 48 h later. Statistical analyses of these data are presented in C) Boxplot of SCR (z-scored) for the early phase of conditioning (Trials 1–2), the late phase (Trials 7–8), and the test trial. Boxes represent the interquartile range, the line indicates the median, whiskers the minimum and maximum values, and each dot corresponds to each individual. Different letters indicate significant differences.
D) Boxplot of stimulus ratings (aversiveness score) before conditioning (Rating 1) and after conditioning (Rating 2) for CS– and CS+. Boxes represent the interquartile range, the line indicates the median, whiskers the minimum and maximum values, and each dot corresponds to each individual. Asterisks indicate significant differences.

Probability and cost

Although no significant differences were found when comparing evaluations (probability and cost) between CS+ and CS−, both in negative and positive situations, a trend emerged toward a more negative evaluation of CS+ compared to CS− in negative situations, but not in positive ones. When comparing differences in the cost ratings of the stimuli across negative and positive situations, it was observed that the aversiveness difference between CS− and CS+ was smaller in negative situations than in positive ones (see Supplementary table 3).

Electroencephalogram (EEG):

In order to evaluate changes in brain activity after the stimulus presentation, power spectrum before (Rest 1) and after (Rest 2) presentation were evaluate for all the channels, 3-30 range frequency and time average (90 seconds). For both experimental groups a positive cluster was found showing and increase of activity after the stimulus.
Reactivation Group: n=26, p=0.0009 (cluster size of 247 data points). Control Group: n=26, p=0.0009. (cluster size of 371 data points). While in the reactivation group the increase in activity during Rest 2 involved most channels, primarily within the 8–23 Hz frequency range, in the control group it occurred between 13 and 30 Hz (Figure 4a).

Based on this information, the next step was to compare post-stimulus brain activity (Rest 2 using Rest 1 as baseline) between conditions within the frequency ranges of interest (8–13 Hz and 25–30 Hz), as these bands showed different results depending on the experimental group.
A negative cluster in the 25–30 Hz frequency range was identified over central regions, reflecting increased oscillatory activity in the control group relative to the reactivation group (n=26, p=0.019, cluster size of 27 data points). Figure 4b,c. No cluster was found for the 8-13 Hz frequency range.

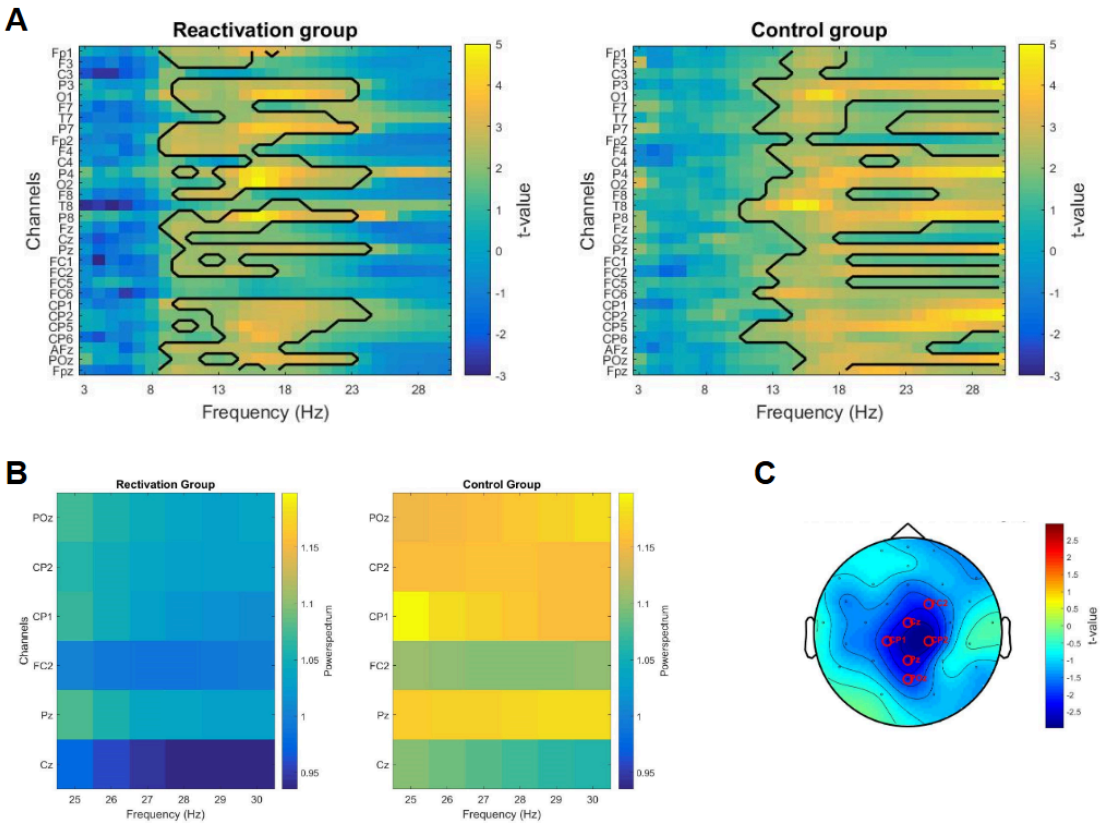

Figure 4. A) t-values from the cluster-based permutation test between Rest 2 and Rest 1 for the Reactivation and Control groups across all channels and frequencies (3–30 Hz). Contours indicate the significant positive cluster for each group.
B) Power spectrum of Rest 2 (baseline-corrected to Rest 1) for the Reactivation and Control groups, restricted to the frequencies and channels where a significant negative cluster was found in the between-group comparison. The spatial distribution of significant channels and the corresponding t-values are shown in C).

Microstates:

After found differences in brain activity between the experimental groups in the power spectrum analysis, we aimed to assess the effect onto the level of transient changes in neural activity states by conducting a microstate analysis.

Global Field Power (GFP)

The GFP (Global Field Power) represents the standard deviation of the voltage amplitude, providing an index of the strength of global activation associated with a given microstate (Poulsen et al., 2018; Tarailis et al., 2024). In the present study, we found higher GFP values during Rest 2 in the control group compared to the reactivation group across all four proposed microstates.
Pairwise comparisons of estimated marginal means revealed that Control was associated with significantly higher GFP values than Reactivation for Microstates C, A, E and B (Microstate C: estimate = 1.12, SE =0.52, t(58) = 2.14, p = 0.036; Microstate A: estimate = 1.07, SE =0.48, t(57) = 2.23, p = 0.029; Microstate E:

estimate = 1.17, SE =0.52, t(58) = 2.24, p = 0.028; Microstate B: estimate = 1.22, SE =0.43, t(61) = 2.82, p = 0.0065). Figure 5a
No differences were found during Rest 1 (see Supplementary table 4)

Global Explained Variance (GEV)

The Global Explained Variance (GEV) reflects how well a given prototype accounts for the data. It is computed as the squared correlation between a sample and its assigned microstate, weighted by the GFP at that specific time point (Poulsen et al., 2018; Tarailis et al., 2024). We found an increase of GEV during Rest 2 only for Microstate C in the Reactivation group (Control group: estimate = -0.011, SE = 0.01, t(48) = -1.12, p = 0.268; Reactivation group: estimate = -0.03, SE =0.01, t(49) = -2.76, p = 0.008) Figure 5b.

Duration

Duration is defined as the average time a given microstate remains active, expressed in milliseconds (Poulsen et al., 2018; Tarailis et al., 2024). Significant differences were found only for microstate A, with the Reactivation group showing longer durations during Rest 2, a difference that was not observed during Rest 1 (Rest1: estimate = -4.49, SE = 3.02, t(73) = -1.48, p = 0.141; Rest 2: estimate = -8.5, SE =3, t(72) = -2.83, p = 0.006). Figure 5c

Coverage

Coverage is defined as the fraction of time a given microstate remains active (Poulsen et al., 2018; Tarailis et al., 2024). Significant differences were found only for microstate E, with the Reactivation group showing a lower coverage during Rest 2 compared with Control group, a difference that was not observed during Rest 1 (Rest1: estimate = 0.042, SE = 0.026, t(59) = 1.64, p = 0.105; Rest 2: estimate = 0.052, SE =0.026, t(58) = 2.03, p = 0.046). Figure 5d

Occurrence

Occurrence reflects the average number of time per second a microstate is dominant (Poulsen et al., 2018; Tarailis et al., 2024). We found a decreased occurrence during Rest 2 only for Microstate E in the Control group (Control group: estimate = 0.19, SE = 0.086, t(50) = 2.22, p = 0.03; Reactivation group: estimate = 0.155, SE =0.084, t(49) = 1.83, p = 0.072) Figure 5e.

Results from the other microstates were present in supplementary table 5.

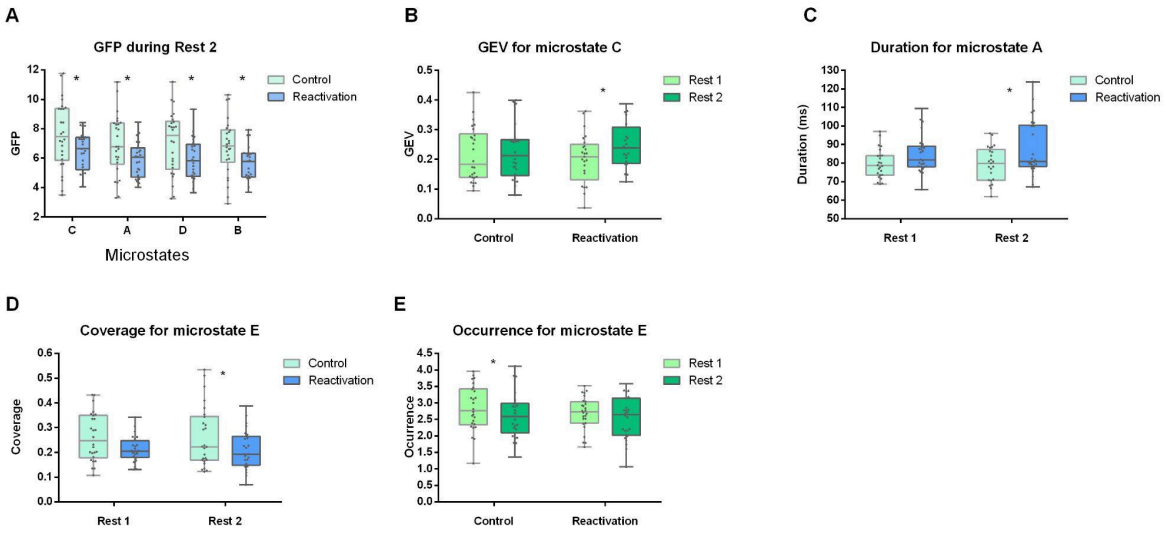

Figure 5. Boxplots showing interquartile range (boxes), median (line), minimum and maximum (whiskers), and individual values (dots) for: A) GFP for the 4 microstates identified in the Reactivation and Control groups. Asterisks indicate significant differences between experimental groups.
B) GEV for microstate C comparing Rest 1 and Rest 2 in both experimental groups. Asterisks indicate significant differences between resting states. C) Duration (ms) for microstate A in each experimental group during Rest 1 and Rest 2. Asterisks indicate significant differences between experimental groups. D) Coverage for microstate E in each experimental group during Rest 1 and Rest 2. E) Occurrence for microstate E comparing Rest 1 and Rest 2 in both experimental groups. Asterisks indicate significant differences between experimental groups and between resting states, respectively.

In the Reactivation group, participants were divided into two subgroups based on behavioral variables: Stimuli representation and SCR. Participants were separated into clusters, which resulted in one group characterized as “good learners,” showing an increased aversiveness score for the CS+ after conditioning and/or a greater SCR to the CS+ than to the CS– following conditioning (cluster 2), and another group characterized as “poor learners,” who did not show an increase in CS+ aversiveness and/or did not exhibit a greater SCR to the CS+ (Cluster 1). Figure 6a

Microstate C:

GFP increased after the reminder in poor learners only, with no change observed in good learners.(poor learners: estimate = -0.535, SE = 0.23, $t(23) = -2.27$, $p = 0.032$; Good learners: estimate = -0.32, SE =0.265, $t(23) = -1.2$, $p = 0.24$). Figure 6b.
GEV increased after the reminder in good learners only, with no change observed in poor learners.(poor learners: estimate = -0.028, SE = 0.022, $t(23) = -1.3$, $p = 0.20$; Good learners: estimate = -0.064, SE =0.024, $t(24) = -2.58$, $p = 0.016$). Figure 6c.

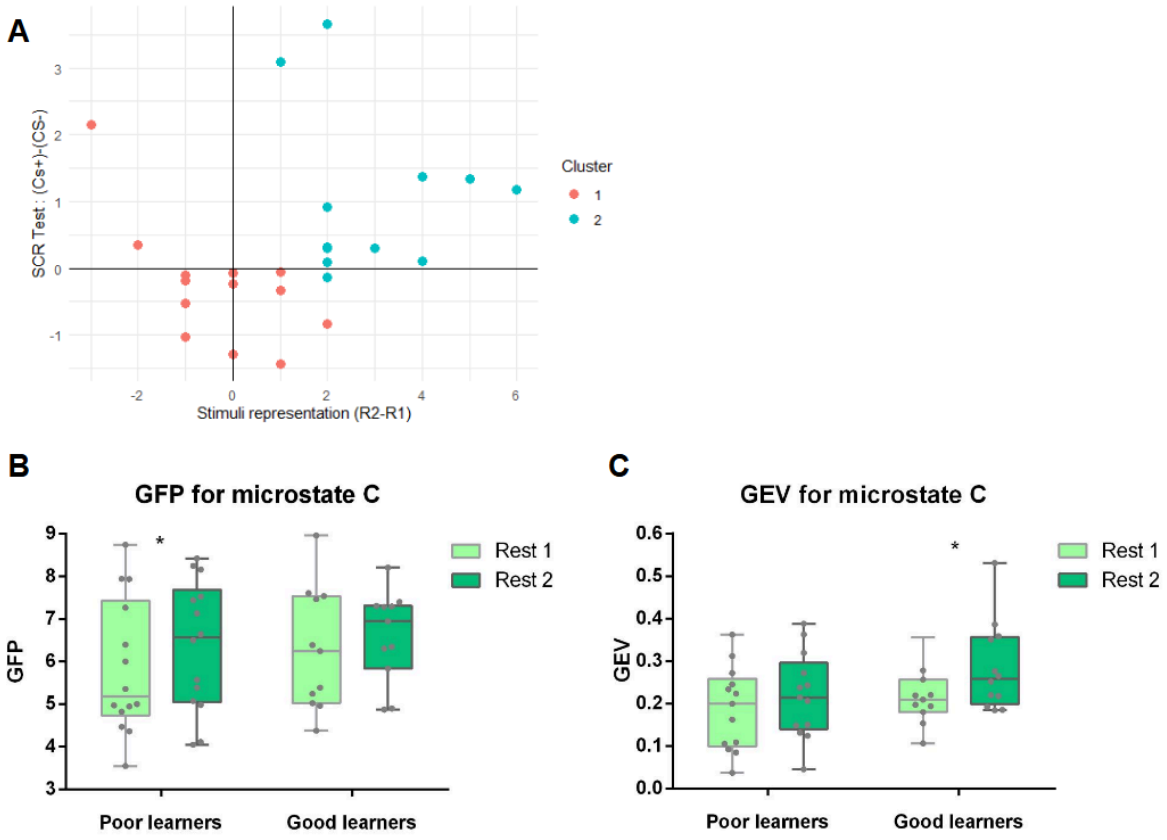

Figure 6.a) Participants were classified into two subgroups using k-means clustering (k = 2) based on standardized differences in evaluative scores and skin conductance responses (CS+ minus CS−) during testing. Cluster 1 was characterized as Poor learners and cluster 2 was characterized as Good learners. b) GFP for microstate C comparing Rest 1 and Rest 2 in Poor and Good learners. Asterisks indicate significant differences between resting states. c) GFP for microstate C comparing Rest 1 and Rest 2 in Poor and Good learners. Asterisks indicate significant differences between resting states.

Discussion

Adaptive behavior requires not only the detection of environmental threats but also the updating of previously acquired information. Memory reactivation facilitates this flexibility by making consolidated memories labile, allowing for modification through reconsolidation (Nader et al., 2000; Fernández et al., 2016). In the current study, we employed a threat-conditioning protocol in which a face (CS+) paired with an aversive tone (US) produced greater skin conductance responses and higher aversiveness ratings compared to non-reinforced stimuli, confirming the success of the conditioning. These findings indicate that threat conditioning activates both physiological and cognitive responses, providing a solid framework for investigating how memory updating mechanisms may facilitate, or hinder, the flexible regulation of aversive memories. Moreover, these results, which combine physiological and declarative measures, underscore the strength of our paradigm and provide an

opportunity to investigate the neural markers associated with post-reactivation memory dynamics.

Previous results (Picco et al, 2022) also demonstrated that the presentation of a reminder containing a prediction error 24 hours after acquisition induces memory labilization. Picco and colleagues found that when participants performed a high-demand cognitive task after reminder presentation (CS+ without US), memory retention was weakened. This effect was explained by competition for the cognitive resources required for both the reconsolidation of the reactivated memory and the demanding task, which ultimately weakened memory. By contrast, when participants performed a low-demand task after reactivation, no such memory impairment was observed. In line with these results,de Voogd and colleagues found that participants exposed to a working memory task showed reduced threat responses and enhanced extinction learning, which could be explained by competition between the salience and central executive networks of the brain (de Voogd and Phelps, 2020)

Based on this evidence, and with the aim of studying the neural activity underlying post-reactivation processes, we recorded EEG activity before and after reminder presentation in two groups: one that had undergone training (the Reactivation group) and another that had not (the Control group).

As previously noted, the amplitude of brain oscillations can provide valuable insights into complex mental processes, with specific oscillatory frequencies associated with particular functions (Lakatos et al., 2005, Klimesch 2018). For instance, Zhu and colleagues utilized MEG to demonstrate a decrease in beta-band activity (15–25 Hz) during the reactivation of episodic memory (Zhu et al., 2019). Likewise, Griffiths and coworkers presented fMRI/EEG evidence suggesting that reductions in alpha/beta activity (8–30 Hz) are associated with enhanced information processing in associative memories (Griffiths et al., 2019). These findings align with the desynchronization hypothesis, which underscores the importance of decreased 8–30 Hz activity during both memory encoding and retrieval (Hanslmayr et al., 2012). According to this hypothesis, desynchronization is linked to a more nuanced representation of information, thereby facilitating both encoding and retrieval.

In line with this framework, we found reduced beta activity (25–30 Hz) in the Reactivation group compared to the Control group, which could be associated with greater post-reactivation processing of the memory, as opposed to participants without prior knowledge of the stimuli. Furthermore, considering that the image presented to the Reactivation group was previously paired with an aversive sound and could therefore trigger the recall of a threatening situation, the observed beta reduction is consistent with MEG results by Roxburgh and coworkers, who reported a decrease in the 14–30 Hz frequency band during periods of threat (unexpectedly delivered electric shocks) (Roxburgh et al., 2023).

In relation to alpha activity (8–13 Hz), we noted an increase in the Reactivation group that was not present in the Control group. However, no significant differences emerged between the two groups. Previous research has suggested that increases in alpha activity are linked to inhibition. Specifically, it has been proposed that regions engaged in a task exhibit decreased alpha activity, while non-involved regions display an increase in alpha, thereby inhibiting potential interference and directing attentional resources (Klimesch, 2012). In episodic memory interference paradigms, an increase in alpha/beta activity (11.5–20 Hz) has been observed in competing memory regions during retrieval, implying that such increases serve to inhibit interference from competing memories (Waldhauser et al., 2012). Given this evidence, the alpha increase seen in the Reactivation group may indicate an inhibition of interference with the reactivated memory. However, due to the lack of significant group differences, we cannot draw any strong conclusions.

It is worth mentioning that many studies report alpha/beta decreases at the time of reactivation, mainly in episodic or working memory paradigms (Hanslmayr et al., 2012, Griffith et al., 2021). In contrast, our study assessed activity during resting-state intervals of 90 seconds, which may reflect not only reactivation itself but also subsequent post-reactivation processes, specifically in the context of threat-conditioning memories.

EEG activity can be described as a dynamic system, with microstates reflecting brief, stable topographies of electrical activity across the scalp. Resting-state EEG, widely used in clinical research, captures spontaneous neural dynamics that may reveal how large-scale brain networks operate (Koenig et al., 2005; Raichle, 2009; Snyder & Raichle, 2012). Building on our spectral analysis of resting-state activity, we complemented this approach with microstate analysis.

Four canonical microstates (A–D) have been consistently described across a wide range of studies and cognitive domains, supporting their role as fundamental units of brain activity (Koenig et al., 2002). In line with this literature, we also identified these canonical microstates in our data (Microstate D sometimes appears as an inverse topography with a posterior-central peak, as in the present work. Nevertheless, following the labels from Tarailis et al. (2024), we label these inverted microstates as E). While microstate analysis has been increasingly applied in psychiatric and neurological disorders, comparatively fewer studies have examined how these patterns relate to specific cognitive processes. In the present study, we aim to contribute evidence on microstate dynamics following the reactivation of threat memories.

Microstate A has been primarily associated with auditory and visual processing; however, some evidence suggests it may also be linked to arousal (Tarailis et al., 2024). Antonova and coworkers found a positive correlation between microstate A duration and self-reported alertness during task performance, which also correlated with increased alpha activity (8–12 Hz) (Antonova et al., 2022). Consistent with this

evidence, we found greater microstate A duration in the Reactivation group, possibly reflecting a higher state of alertness due to the association between the CS+ and the aversive US.

Microstate E has been associated with emotional information processing and alertness (Tarailis et al., 2024; Zanesco et al., 2020). In particular, its coverage has been negatively correlated with somatic awareness (Pipinis et al., 2017; Tarailis et al., 2021). In our study, we found reduced microstate E coverage in the Reactivation group, which may also be related to a heightened state of alertness due to anticipation of the aversive sound. However, because occurrence decreased only in the Control group, the effect of reactivation on microstate E should be interpreted with caution.

Given that microstate C accounts for the greatest proportion of total variance, we focused our analysis of behavioral correlations on this microstate. Based on fMRI, EEG, and brain stimulation evidence, microstate C has been proposed to reflect the default mode network (DMN) (Croce et al., 2018; Brechet et al., 2019; Tarailis et al., 2024). The DMN is a network of interconnected brain regions, whose decreased activity has been linked to externally focused attention, whereas it is typically active during mind wandering or resting states (Raichle et al., 2001; Buckner et al., 2008; Menon, 2023).

In our study, GFP was greater in the Control group across microstates. In particular, the reduced microstate C activity in the Reactivation group could be related to the focus on a salient stimulus, whereas greater activity in the Control group may reflect mind wandering after the presentation of a stimulus without associated information. Interestingly, when we further subdivided the Reactivation group into two clusters based on their physiological responses (SCR) and cognitive biases, we identified “good learners” (showing stronger CS+ than CS- responses after conditioning) and “poor learners” (who showed weaker or absent effects). In poor learners, the CS+ was likely less salient, and these participants exhibited increased post-stimulus GFP in microstate C, possibly reflecting mind wandering. By contrast, good learners did not show this increase, consistent with greater focus on the stimulus. These findings are further supported by GEV analyses, which revealed increased variance explained by microstate C only in the Reactivation group, primarily driven by good learners who exhibited the same pattern. This analysis allows us to evaluate differences in microstates between groups separated according to their behavior, not only through the implicit response but also by incorporating cognitive biases

Taken together, our results suggest that beta-band activity (25–30 Hz) in central regions plays a crucial role in the post-reactivation processes of threat-conditioning memories, as its reduction is observed. Furthermore, microstate A appeared to be active for a longer duration following memory reactivation, and we propose a potential role for microstate E, although further studies are needed to clarify this. Finally, we suggest that increased microstate C power in the Control group reflects

periods of mind wandering, while the correlation between this microstate and behavioral results suggests that the reminder is more salient in participants who exhibit clearer signs of learning and memory.

limitation: It is important to note that although the primary objective of our study was to assess the reactivation of threat memories, we cannot completely rule out the potential effect of episodic memory reactivation triggered by exposure to a context similar to that of the previous day.

Reference

Alberini, C. M. (2005). Mechanisms of memory stabilization: are consolidation and reconsolidation similar or distinct processes?. Trends in neurosciences, 28(1), 51-56.

Antonova, E., Holding, M., Suen, H. C., Sumich, A., Maex, R., & Nehaniv, C. (2022). EEG microstates: functional significance and short-term test-retest reliability. Neuroimage: Reports, 2(2), 100089.

Beck, A. T., Steer, R. A., Epstein, N., & Brown, G. (1990). Beck self-concept test. Psychological Assessment: A Journal of Consulting and Clinical Psychology, 2(2),191.

Boddez, Y., Vervliet, B., Baeyens, F., Lauwers, S., Hermans, D., & Beckers, T. (2012). Expectancy bias in a selective conditioning procedure: Trait anxiety increases the threat value of a blocked stimulus. Journal of behavior therapy and experimental psychiatry, 43(2), 832-837.

Braithwaite, J. J., Watson, D. G., Jones, R., & Rowe, M. (2013). A guide for analysing electrodermal activity (EDA) & skin conductance responses (SCRs) for psychological experiments. Psychophysiology, 49(1), 1017-1034.

Bréchet, L., Brunet, D., Birot, G., Gruetter, R., Michel, C. M., & Jorge, J. (2019). Capturing the spatiotemporal dynamics of self-generated, task-initiated thoughts with EEG and fMRI. Neuroimage, 194, 82-92.

Browning, M., Behrens, T. E., Jocham, G., O'Reilly, J. X., & Bishop, S. J. (2015). Anxious individuals have difficulty learning the causal statistics of aversive environments. Nature neuroscience

Buckner, R. L., Andrews-Hanna, J. R., & Schacter, D. L. (2008). The brain's default network: anatomy, function, and relevance to disease. Annals of the new York Academy of Sciences, 1124(1), 1-38.

Croce, P., Zappasodi, F., & Capotosto, P. (2018). Offline stimulation of human parietal cortex differently affects resting EEG microstates. Scientific Reports, 8(1), 1287.

Davis, M. (1992). The role of the amygdala in fear and anxiety. Annual review of neuroscience, 15(1), 353-375.

de Voogd, L. D., & Phelps, E. A. (2020). A cognitively demanding working-memory intervention enhances extinction. Scientific Reports, 10(1), 7020.

Fanselow, M. S. (2018). The role of learning in threat imminence and defensive behaviors. Current opinion in behavioral sciences, 24, 44-49.

Fanselow, M. S., & Poulos, A. M. (2005). The neuroscience of mammalian associative learning. Annual review of psychology, 56(1), 207-234.

Fernández, R. S., Boccia, M. M., & Pedreira, M. E. (2016). The fate of memory: reconsolidation and the case of prediction error. Neuroscience & Biobehavioral Reviews, 68, 423-441.

Fernández, R. S., Picco, S., Messore, F., & Pedreira, M. E. (2018). Effects of Threat Conditioning on the Negative Valanced Systems and Cognitive Systems. Scientific Reports, 8

Forcato, C., Argibay, P. F., Pedreira, M. E., & Maldonado, H. (2009). Human reconsolidation does not always occur when a memory is retrieved: the relevance of the reminder structure. Neurobiology of learning and memory, 91(1), 50-57.

Griffiths, B. J., Mayhew, S. D., Mullinger, K. J., Jorge, J., Charest, I., Wimber, M., & Hanslmayr, S. (2019). Alpha/beta power decreases track the fidelity of stimulus-specific information. elife, 8, e49562.

Griffiths, B. J., Martín-Buro, M. C., Staresina, B. P., Hanslmayr, S., & Staudigl, T. (2021). Alpha/beta power decreases during episodic memory formation predict the magnitude of alpha/beta power decreases during subsequent retrieval. Neuropsychologia, 153, 107755.

Grillon, C. (2002). Startle reactivity and anxiety disorders: aversive conditioning, context, and neurobiology. Biological psychiatry, 52(10), 958-975.

Grupe, D. W., & Nitschke, J. B. (2013). Uncertainty and anticipation in anxiety: an integrated neurobiological and psychological perspective. Nature Reviews Neuroscience, 14(7), 488-501.

Hanslmayr, S., Staudigl, T., & Fellner, M. C. (2012). Oscillatory power decreases and long-term memory: the information via desynchronization hypothesis. Frontiers in human neuroscience, 6, 74.

Kindt, M., Soeter, M., & Vervliet, B. (2009). Beyond extinction: erasing human fear responses and preventing the return of fear. Nature neuroscience, 12(3), 256-258.

Klimesch, W. (2012). Alpha-band oscillations, attention, and controlled access to stored information. Trends in cognitive sciences, 16(12), 606-617.

Klimesch, W. (2018). The frequency architecture of brain and brain body oscillations: an analysis. European Journal of Neuroscience, 48(7), 2431-2453.

Koenig, T., Prichep, L., Lehmann, D., Sosa, P. V., Braeker, E., Kleinlogel, H., ... & John, E. R. (2002). Millisecond by millisecond, year by year: normative EEG microstates and developmental stages. Neuroimage, 16(1), 41-48.

Koenig, T., Studer, D., Hubl, D., Melie, L., & Strik, W. K. (2005). Brain connectivity at different time-scales measured with EEG. Philosophical Transactions of the Royal Society B: Biological Sciences, 360(1457), 1015-1024.

Lakatos, P., Shah, A. S., Knuth, K. H., Ulbert, I., Karmos, G., & Schroeder, C. E. (2005). An oscillatory hierarchy controlling neuronal excitability and stimulus processing in the auditory cortex. Journal of neurophysiology, 94(3), 1904-1911.

LeDoux, J. E. (2000). Cognitive-emotional interactions. Cognitive neuroscience of emotion, 129-155.

Lehmann, D., Ozaki, H., & Pál, I. (1987). EEG alpha map series: brain micro-states by space-oriented adaptive segmentation. Electroencephalography and clinical neurophysiology, 67(3), 271-288.

Lehmann, D. (1990). Brain electric microstates and cognition: the atoms of thought. In Machinery of the mind: data, theory, and speculations about higher brain function (pp. 209-224). Boston, MA: Birkhäuser Boston.

Leung, C. J., Yiend, J., Trotta, A., & Lee, T. M. (2022). The combined cognitive bias hypothesis in anxiety: A systematic review and meta-analysis. Journal of anxiety disorders, 89, 102575.

Lissek, S., Powers, A. S., McClure, E. B., Phelps, E. A., Woldehawariat, G., Grillon, C., & Pine, D. S. (2005). Classical fear conditioning in the anxiety disorders: a meta-analysis. Behaviour research and therapy, 43(11), 1391-1424.

Menon, V. (2023). 20 years of the default mode network: A review and synthesis. Neuron, 111(16), 2469-2487.

Milad, M. R., & Quirk, G. J. (2012). Fear extinction as a model for translational neuroscience: ten years of progress. Annual review of psychology, 63(1), 129-151.

Nader, K., Schafe, G. E., & Le Doux, J. E. (2000). Fear memories require protein synthesis in the amygdala for reconsolidation after retrieval. Nature, 406(6797), 722-726.

Oostenveld, R., Fries, P., Maris, E., & Schoffelen, J. M. (2011). FieldTrip: open source software for advanced analysis of MEG, EEG, and invasive electrophysiological data. Computational intelligence and neuroscience, 2011(1), 156869.

Öhman, A., & Mineka, S. (2001). Fears, phobias, and preparedness: toward an evolved module of fear and fear learning. Psychological review, 108(3), 483.

Phelps, E. A., & LeDoux, J. E. (2005). Contributions of the amygdala to emotion processing: from animal models to human behavior. Neuron, 48(2), 175-187.

Pipinis, E., Melynyte, S., Koenig, T., Jarutyte, L., Linkenkaer-Hansen, K., Ruksenas, O., & Griskova-Bulanova, I. (2017). Association between resting-state microstates and ratings on the Amsterdam resting-state questionnaire. Brain topography, 30(2), 245-248.

Picco, S., Bavassi, L., Fernandez, R. S., & Pedreira, M. E. (2022). Highly Demand Working Memory Intervention Weakens a Reactivated Threat Memory and the Associated Cognitive Biases. Neuroscience, 497, 257-270.

Poulsen, A. T., Pedroni, A., Langer, N., & Hansen, L. K. (2018). Microstate EEGlab toolbox: An introductory guide. BioRxiv, 289850

Raichle, M. E., MacLeod, A. M., Snyder, A. Z., Powers, W. J., Gusnard, D. A., & Shulman, G. L. (2001). A default mode of brain function. Proceedings of the national academy of sciences, 98(2), 676-682.

Raio, C. M., Carmel, D., Carrasco, M., & Phelps, E. A. (2012). Nonconscious fear is quickly acquired but swiftly forgotten. Current Biology, 22(12), R477-R479.

Rogan, M. T., Stäubli, U. V., & LeDoux, J. E. (1997). Fear conditioning induces associative long-term potentiation in the amygdala. Nature, 390(6660), 604-607.

Roxburgh, A. D., White, D. J., Grillon, C., & Cornwell, B. R. (2023). A neural oscillatory signature of sustained anxiety. Cognitive, Affective, & Behavioral Neuroscience, 23(6), 1534-1544.

Sjouwerman, R., & Lonsdorf, T. B. (2019). Latency of skin conductance responses across stimulus modalities. Psychophysiology, 56(4), e13307.

Snyder, A. Z., & Raichle, M. E. (2012). A brief history of the resting state: the Washington University perspective. Neuroimage, 62(2), 902-910.

Waldhauser, G. T., Johansson, M., & Hanslmayr, S. (2012). Alpha/beta oscillations indicate inhibition of interfering visual memories. Journal of Neuroscience, 32(6), 1953-1961.

Zhu, Z., Wang, Y., Jia, J., & Wu, Y. (2019). Beta and alpha desynchronizations underlie reconsolidation-mediated episodic memory updating. Neuropsychologia, 132, 107135.

Spielberger, C. D. (1970). Manual for the State-Trait Anxiety Inventory (self-evaluation questionnaire). (No Title). https://cir.nii.ac.jp/crid/1370285712575158016

Tarailis, P., Šimkutė, D., Koenig, T., & Griškova-Bulanova, I. (2021). Relationship between spatiotemporal dynamics of the brain at rest and self-reported spontaneous thoughts: an EEG microstate approach. Journal of personalized medicine, 11(11), 1216

Tarailis, P., Koenig, T., Michel, C. M., & Griškova-Bulanova, I. (2024). The functional aspects of resting EEG microstates: a systematic review. Brain topography, 37(2), 181-217.

Tversky, A., & Kahneman, D. (1974). Judgment under Uncertainty: Heuristics and Biases: Biases in judgments reveal some heuristics of thinking under uncertainty. science, 185(4157), 1124-1131.

Zanesco, A. P., King, B. G., Skwara, A. C., & Saron, C. D. (2020). Within and between-person correlates of the temporal dynamics of resting EEG microstates. NeuroImage, 211, 116631.

Supplementary material

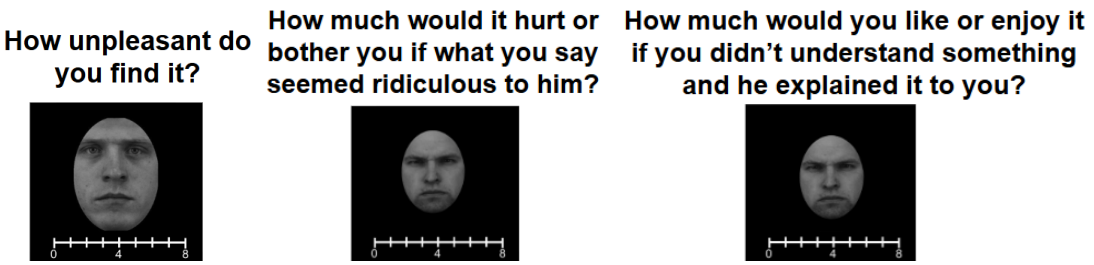

Supplementary Figure 1. A) Twelve different male faces (seven angry and five neutral) were presented on a screen with a 0–8 aversiveness scale; one of the faces is shown as an example. B) A negative scenario and C) a positive scenario were presented with the face; CS− is shown as an example

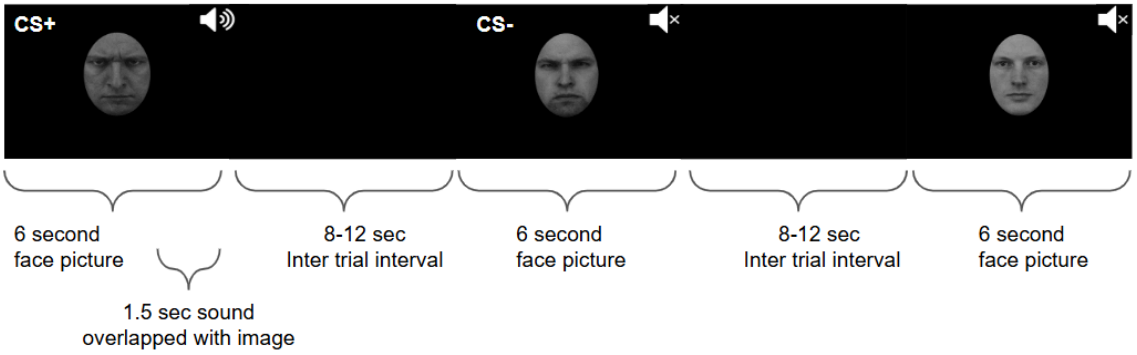

CS-	CS n	CS+	CS-	CS+	CS-	CS n	CS+	CS n	CS-	CS n	CS+	CS+	CS n	CS-	CS+	CS-	CS n	CS+	CS-	CS n	CS n	CS+	CS-

CS-	CS+	CS n	CS-	CS-	CS n	CS+	CS-	CS+	CS n	CS n	CS-	CS+	CS n	CS+	CS-	CS n	CS-	CS+	CS+	CS n	CS-	CS n	CS+
CS n	CS n	CS-	CS+	CS n	CS+	CS-	CS n	CS-	CS+	CS-	CS n	CS-	CS+	CS n	CS+	CS-	CS+	CS n	CS+	CS-	CS+	CS n	CS-
CS-	CS n	CS+	CS-	CS+	CS n	CS+	CS-	CS n	CS-	CS+	CS n	CS+	CS-	CS n	CS+	CS n	CS-	CS+	CS n	CS-	CS-	CS+	CS n

Supplementary Figure 2. The three faces used as CSs (CS+ and CS− pictures were counterbalanced across participants). During acquisition, each face was presented eight times in a different order. Four different combinations were used. The CS+ in red corresponds to the CS+ not paired with the US.:

	acquisition	Test statistic	P-value
Shapiro-Wilk normality test	Early phase	w=0.97	p-value=0.367
Mauchly test for sphericity	Early phase	0.78	p-value=0.097
Levene`s test for homogeneity of variance	Early phase	f-value= 1.12	p-value=0.33
Shapiro-Wilk normality test	Late phase	w=0.97	p-value=0.472
Mauchly test for sphericity	Late phase	0.93	p-value=0.474
Levene`s test for homogeneity of variance	Late phase	f-value= 0.24	p-value=0.78
	Memory test		
Shapiro-Wilk normality test	Test	w=0.95	p-value=0.082
Mauchly test for sphericity	Test	0.96	p-value=0.708
Levene`s test for homogeneity of variance	Test	f-value= 2.58	p-value=0.082

Supplementary Table 1. Test statistics and p-values for the assumptions of the implicit response during the early and late phases of acquisition and the memory retention test.

Variable	Test	Likelihood Ratio Test	p-value
Time and Stimulus	Multicollinearity VIF=1		
Time	Proportional odds assumption	10.57	0.158
Stimulus	Proportional odds assumption	7.20	0.074

Supplementary Table 2. Test statistics and p-values for the assumptions of cognitive biases. Variance Inflation Factors (VIFs) are reported for the multicollinearity assumption, and the likelihood ratio test (LRT) and p-values are reported for the proportional odds assumption

Valuation	Comparison	Estimate	SE	Z ratio	p-value
Negative Probability	CS+ vs CS-	0.38	0.16	2.41	0.074
Positive Probability	CS+ vs CS-	-0.08	0.16	-0.54	0.949
Negative Cost	CS+ vs CS-	0.32	0.16	1.91	0.213
Positive Cost	CS+ vs CS-	-0.32	0.15	-2.12	0.14
Positive and Negative Cost	Negative vs Positive	-0.833	0.336	-2.47	0.022

Supplementary Table 3. Test statistics and p-values for the comparison between CS+ and CS− for negative and positive scenarios (Probability and Cost), as well as for the comparison between negative and positive Cost (differences between CS+ and CS− for each Cost)

Microstate		Estimate	SE	t-value	p-value
C	GFP rest1	0.93	0.52	(58)=1.78	0.083
A	GFP rest1	0.72	0.48	(57)=1.5	0.130
E	GFP rest1	0.78	0.52	(58)=1.5	0.139
B	GFP rest1	0.69	0.43	(60)=1.6	0.116

Supplementary Table 4. Test statistics and p-values for the comparison of Global Field Power between the Reactivation and Control groups during Rest 1.

Microstate	GEV Control	Estimate	SE	t-value	p-value
A	R1 vs R2	0.0073	0.0055	(43)=1.3	0.194
E	R1 vs R2	-0.0035	0.0069	(47)=-0.5	0.57
B	R1 vs R2	-0.0076	0.0046	(47)=-1.63	0.108
Microstate	GEV Reactivation	Estimate	SE	t-value	p-value
A	R1 vs R2	0.0024	0.0061	(45)=0.399	0.691
E	R1 vs R2	0.0034	0.0074	(47)=0.46	0.643
B	R1 vs R2	-0.0017	0.0047	(47)=-0.37	0.708

Microstate	Duration R1	Estimate	SE	t-value	p-value
C	Control vs Reactivation	5.08	7.00	(61)=0.72	0.47
E	Control vs Reactivation	5.51	4.09	(67)=1.348	0.18
B	Control vs Reactivation	0.33	2.46	(77)=0.135	0.892
Microstate	Duration R2	Estimate	SE	t-value	p-value
C	Control vs Reactivation	4.04	7.02	(62)=0.57	0.56
E	Control vs Reactivation	6.48	4.06	(67)=1.59	0.115
B	Control vs Reactivation	-0.32	2.46	(77)=-0.13	0.897

Microstate	Coverage R1	Estimate	SE	t-value	p-value
C	Control vs Reactivation	0.0036	0.029	(62)=0.125	0.9
A	Control vs Reactivation	-0.026	0.018	(62)=-1.42	0.15
B	Control vs Reactivation	-0.019	0.015	(61)=-1.26	0.21

Microstate	Coverage R2	Estimate	SE	t-value	p-value
C	Control vs Reactivation	-0.0067	0.029	(62)=-0.22	0.81
A	Control vs Reactivation	-0.036	0.018	(62)=-1.92	0.06
B	Control vs Reactivation	-0.008	0.015	(62)=-0.53	0.59

Microstate	Occurrence Control	Estimate	SE	t-value	p-value
C	R1 vs R2	-0.03	0.09	(50)=2.42	0.019
A	R1 vs R2	0.219	0.0069	(47)=-0.5	0.57
B	R1 vs R2	0.04	0.078	(50)=0.56	0.57
Microstate	Occurrence Reactivation	Estimate	SE	t-value	p-value
C	R1 vs R2	0.2	0.09	(50)=2.21	0.03
A	R1 vs R2	0.0034	0.0074	(47)=0.46	0.643
B	R1 vs R2	0.113	0.07	(50)=1.44	0.15

Supplementary Table 5. Test statistics and p-values for the remaining microstate comparisons not shown in the main text.